Influence of Mashed Potato Dielectric Properties and Circulating Water Electric Conductivity on Radio Frequency Heating at 27 MHz

Jian Wang[1], Robert G. Olsen[2], Juming Tang[1*] and Zhongwei Tang[1]

[1] Dept. of Biological Systems Engineering, Washington State University, Pullman, WA, USA
[2] School of Electrical Engineering and Computer Science, College of Engineering and Architecture, Washington State University, Pullman, WA, USA
[*] *jtang@wsu.edu*

Experiments and computer simulations were conducted to systematically investigate the influence of mashed potato dielectric properties and circulating water electric conductivity on electromagnetic field distribution, heating rate, and heating pattern in packaged food during radio frequency (RF) heating processes in a 6 kW, 27 MHz laboratory scale RF heating system. Both experimental and simulation results indicated that for the selected food (mashed potato) in this study, the heating rate decreased with an increase of electric conductivity of circulating water and food salt content. Simplified analytical calculations were carried out to verify the simulation results, which further indicated that the electric field distribution in the mashed potato samples was also influenced by their dielectric properties and the electric conductivity of the surrounding circulating water. Knowing the influence of water electric conductivity and mashed potato dielectric properties on the heating rate and heating pattern is helpful in optimizing the radio frequency heating process by properly adjusting these factors. The results demonstrate that computer simulation has the ability to demonstrate influence on RF heat pattern caused by the variation of material physical properties and the potential to aid the improvement on construction and modification of RF heating systems.

Submission Date: 18 October 2007
Acceptance Date: 12 March 2008
Publication Date: 11 June 2008

INTRODUCTION

Sterilization is used to reduce spoilage, eliminate pathogenic microorganisms, and prolong the shelf-life of packaged foods. Conventional sterilizing methods such as steam retorting are time consuming. Since the surface of packaged food is normally exposed to high temperatures for a long period of time, the food quality degradation at the container periphery is severe, especially for heat-sensitive foods [Meredith, 1998; Priestley, 1979]. Thermal processes that utilize high temperatures for short duration can produce a better quality food product while ensuring food safety [Banwart, 1989]. Radio frequency (RF) heating has this potential. It may also use less energy than conventional processes. As such,

Keywords: *Computer simulation, dielectric properties, finite element method, numerical modeling, radio frequency heating, radio frequency sterilization, thermal processing*

it may be an improved means for producing higher quality, shelf-stable foods for civilian and military uses [Wang *et al*., 2003a]. Since power penetration depths in the RF range are several times deeper than at microwave frequencies, RF heating has an obvious advantage to process institutional-size packaged food over microwave heating [Wang *et al*., 2003b]. Previous works involving inoculated pack studies and instrumental quality measurements reveal that sterilization using RF energy can produce shelf-stable foods with better quality than retort-treated food products in large polymeric trays [Luechapattanaporn *et al*., 2004; 2005].

Although RF heating processes have several advantages over conventional and microwave heating processes, we are still facing challenges in determining the positions of cold and hot spots in packaged foods and in improving heating uniformity. Both challenges are related to the electromagnetic field distribution within dielectric heating equipment. In early studies, determination of the electromagnetic field distribution and heating pattern associated with RF heating was mainly based on experiments.

Lengthy experimentation times, high operational costs, and lack of flexibility are inherent problems in experimental research. With the rapid development of numerical simulation techniques, computer modeling has great potentials in predicting electromagnetic field distribution and heating patterns inside heating oven and foods. Several previous studies were conducted to numerically simulate RF heating processes. Neophytou and Metaxas [1998; 1999] demonstrated the capability of the finite element method (FEM) for modeling an RF heating system, they suggested the possibility of simulating an entire RF heating system with both generator and applicator circuits, thus opened opportunity for analyzing the structure and circuit design of an RF heating system to optimize its effectiveness via tuning and design of the RF heating system. Chan *et al*. [2004] predicted RF heating patterns in foods due to electromagnetic field distribution. Baginski *et al*. [1990] and Marshall and Metaxas [1998] showed the potential of computer simulation to model RF drying processes and the associated electromagnetic and thermodynamic phenomena. However, few systematic studies have focused on the specific application of RF energy to food sterilization processes nor on the influence of variation in food dielectric properties and electric conductivity of circulating water that used to mitigate the fringing field and edge heating effects, leading to a lack of information electromagnetic field distribution, heating rate, and heating patterns in packaged foods during RF heating.

Thermal effects analysis, besides electromagnetic field investigation, is essential for simulating RF heating processes. During RF heating, two physical factors, temperature and electric field intensity, interrelate with each other. In particular, the dissipated energy provided by electric fields heats those materials with temperature-dependent dielectric properties. The variation, caused by temperature change and heat transfer of the dielectric properties, influences the electromagnetic field distribution. So the coupling of two physical phenomena becomes one of the most critical factors for the successful simulation of RF heating process (i.e., requires software with the ability to handle multiphysical problems).

The objectives of this research were to 1) investigate the influence of the electric conductivity of circulating water and dielectric properties of mashed potatoes on the food s heating rate and pattern, and 2) simulate RF heating processes using commercial simulation software (COMSOL Multiphysics, Burlington, MA). COMSOL Multiphysics, a modeling package for the simulation of physical processes that can be described with partial differential equations, enabled the modeling and coupling of the electric field distribution and heat transfer phenomena through predefined modeling templates [COMSOL, 2005].

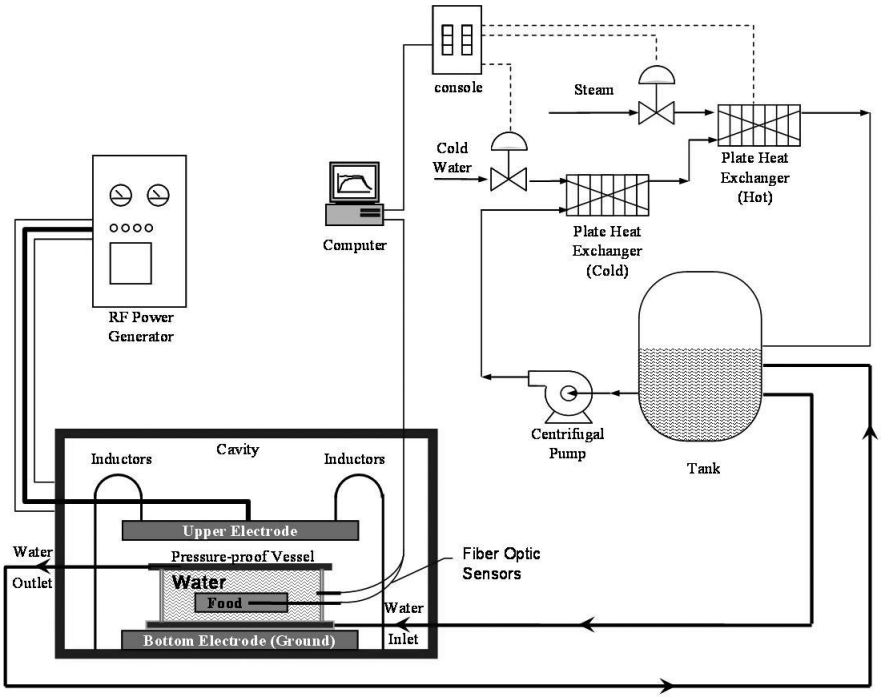

Figure 1. *Simplified schematic diagram of the Washington State University RF heating system.*

EXPERIMENTAL PROCEDURES

Materials and Experimental Procedures

A simplified schematic diagram of the pilot-scale 6 kW 27 MHz RF heating system used in the experiments is shown in Figure 1. The system consists of a RF power generator, an applicator, a pressure-proof vessel to hold packaged foods (Figure 2), a water conditioning system, a temperature monitoring system, and a data collecting system.

The water conditioning system consisting of buffer tanks, heat exchangers, pumps and connecting pipers was used to circulate water through the pressure-proof vessel and adjust the electric conductivity, pressure, temperature, and flow rate of circulating water. The circulating water was used to improve the heating uniformity in the sample food, including reduction of edge heating.

The pressure-proof vessel (as shown in Figure 2) was developed at Washington State University (Pullman, WA, USA) to provide an overpressure of up to 0.276 MPa (40 psi) that allowed foods in large polymeric trays to be heated up to 135˚C without bursting. The vessel was constructed with Ultem (polyetherimide, or PEI) plastic walls and 2 parallel aluminum plates as upper and lower covers. Several probe ports were drilled on one side of the wall to allow insertion of fiber optic sensors (UMI; FISO Technologies Inc., Quebec, Canada) that were used to detect the real-time temperatures of the food samples. A computer was used to record the data measured by the sensors.

The dielectric properties of mashed potatoes were adjusted by changing salt content. Mashed potato samples consisted of mashed potato flakes (from Oregon Potato Co., Broadman, OR., USA), deionized water, and table salt (NaCl). Non-salted samples consisted of mashed potato flakes and deionized water at 5.5:1 water/potato mass ratios; the corresponding moisture content was 85.9% (wet basis), with a 0.8% (w.b.) salt content. Salt-enriched samples had the same moisture content, but by adding salt solution with 0.63% salt concentration, samples had a 1.3% (w.b.) salt content.

About 2600 g of mashed potatoes samples

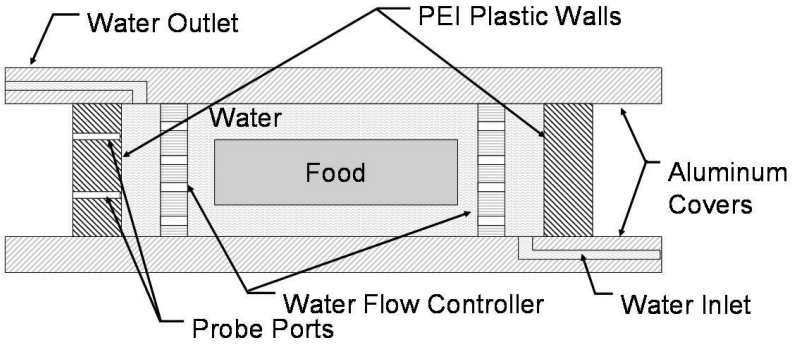

Figure 2. *Diagram of the pressure-proof vessel cross section (not to scale).*

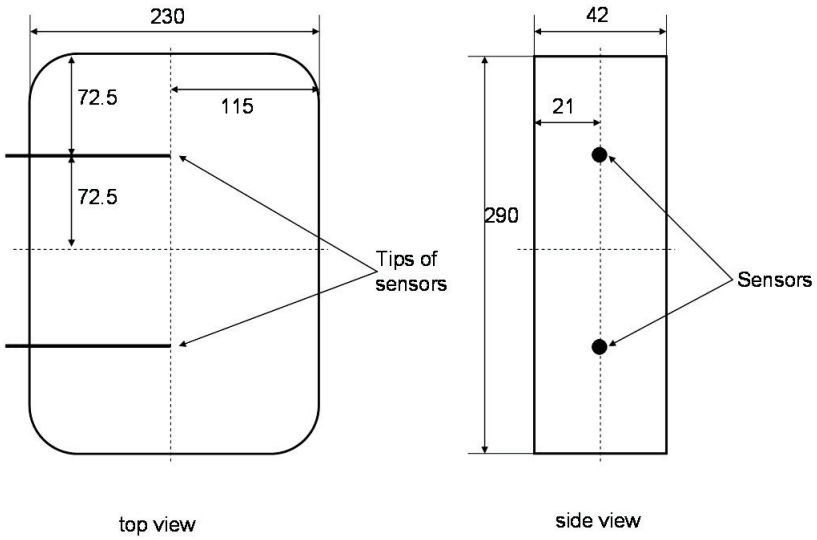

Figure 3. *Positions of fiber optic sensors in the tray (units in the figure are mm).*

were filled in each of 6-pound capacity polymeric trays (295 · 235 · 42 mm) commonly used as packages for U.S. military group rations. The trays were heat-sealed under about 61 kPa (18 in Hg) below atmospheric vacuum with a 0.15-mm-thick aluminum foil lid (Jefferson Smurfit, Dublin, Ireland) in a laboratory vacuum tray sealer (Rexam Containers, Union, MO, USA). The trays were then placed in the pressure-proof vessel positioned at the center of the bottom plate in the RF heating oven. Circulating water was pumped through the vessel before and during the heating process. The inlet temperature of the circulating water was controlled by the water conditioning system. During RF processing, the flow rate of the circulating water was controlled at approximately 10 L/min, the pressure at 13.8 kPa (2 psi), and the temperature at 40 °C. Two fiber optic sensors, placed in the sample trays as illustrated in Figure 3, were used to monitor the sample temperatures at sensor tips. The average temperature of the two sensors was used to characterize the heating rate.

Immediately after each test run, the sample trays were removed from the pressure-proof vessel and thermal images at the intersection of the horizontal plane, in which fiber optic sensors were placed, were taken by a ThemaCAM infrared camera (FLIR System Inc., Sweden) that had been set up and calibrated before the

experiment. Temperature differences at random positions checked by the thermal images and a thermocouple were controlled within ± 1 °C. It normally took 3 to 4 min from turning off the RF power to take the thermal image. Four different circulating water electrical conductivities, 20, 64, 140, and 220 μS/cm at 23°C were used.

NUMERICAL MODEL

Figure 4 illustrates computer simulation procedures. An appropriate simulation module was chosen based on governing equations that revealed the physical basis of simulated physical phenomena. The constants and variables were then predefined. After the geometry of the model was built, the sub-domain properties and boundary conditions were assigned. A convergence study was conducted to investigate convergence of the simulation and to determine the optimized meshing that comprises the calculation time and accuracy of simulation. Finally, the computing solution was calculated and the simulation results were analyzed.

Assumptions

In order to accomplish the simulation with acceptable accuracy under the constrained memory capability of the computer, assumptions were used to simplify the heating system. A quasi-static analysis was assumed because the wavelength of the electromagnetic wave (27 MHz) in our research (> 10 m in air and > 1.5 m in food) was much larger than the dimension of our equipment (< 1 m) and food (< 0.3 m). In addition, the flow of circulating water inside the pressure-proof vessel and the heat transfer between the circulating water and food were neglected because we concentrated on the heating distribution at the center layer of the sample trays; the influence from the circulating water was small.

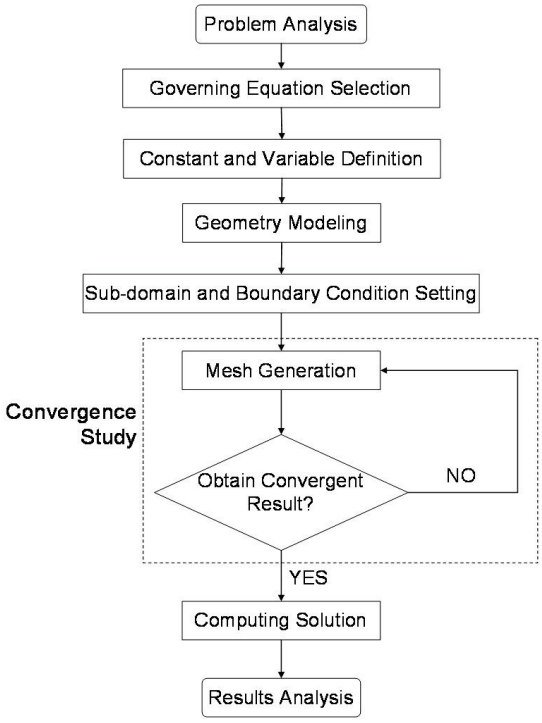

Figure 4. *Flow chart of the computer simulation procedure.*

Governing equations

The electromagnetic field patterns in RF systems are governed by Maxwell s equations [Balanis, 1989]:

$$\nabla \cdot \boldsymbol{H} = \sigma \boldsymbol{E} + \frac{\partial(\varepsilon \boldsymbol{E})}{\partial t} \tag{1}$$

$$\nabla \cdot \boldsymbol{E} = -\frac{\partial \boldsymbol{B}}{\partial t} = -\frac{\partial(\mu \boldsymbol{H})}{\partial t} \tag{2}$$

$$\nabla \cdot \boldsymbol{D} = \nabla \cdot \varepsilon \boldsymbol{E} = 0 \tag{3}$$

$$\nabla \cdot \boldsymbol{B} = \nabla \cdot \mu \boldsymbol{H} = 0 \tag{4}$$

where $\boldsymbol{E}$ is electric field intensity, $\boldsymbol{H}$ is magnetic field intensity, $\boldsymbol{D}$ is electric flux density, $\boldsymbol{B}$ is magnetic field density, and ε and μ are, respectively, dielectric constant and permeability of the material.

Electroquasistatic analysis is applicable when the coupling between electric and magnetic fields is negligible under the condition that that all dimensions are small compared to the wavelength in any relevant medium. A more complete discussion of the conditions under which this simplification can be made can be found in Haus and Melcher [1989]. Therefore

$$\nabla \cdot \boldsymbol{E} = -\frac{\partial \boldsymbol{B}}{\partial t} = 0 \tag{5}$$

Hence, $\boldsymbol{E}$ can be derived from a scalar electric potential V as:

$$\boldsymbol{E} = -\nabla V \tag{6}$$

Therefore, Eq. (6) can be rearranged as:

$$\nabla^2 V = 0 \tag{7}$$

which is Laplace's equation.

In our simulation, by solving Eq. (7), the electric potential (V) and electric field intensity ($\boldsymbol{E}$) were obtained.

Note that the time interval over which the power is calculated (one cycle of the electromagnetic field) is less than 0.04 μSec (27 MHz). According to two-time-scale approach, the time interval is very small compared to the thermal changes, it can be used as a time varying quantity, $P(t)$, in the thermal problem.

The dielectric properties of food materials can be described as [Sadiku, 2001]:

$$\varepsilon_c = \varepsilon - j\varepsilon'' = \varepsilon_0(\varepsilon_r' - j\varepsilon_r'') \tag{8}$$

where, ε_c is complex permittivity of the material, ε_0 is permittivity of free space, ε_r' is relative dielectric constant, and ε_r'' is relative loss factor of the material. Considering at 27 MHz ε_r'' can be approximated as:

$$\varepsilon_r'' = \frac{\sigma}{\omega \varepsilon_o} \tag{9}$$

where σ is electrical conductivity of the material.

The time-averaged power density, P, was generated by transferring the electric energy to heat the food material as shown by [Barber, 1983]:

$$P = \varepsilon_0 \varepsilon_r'' \omega \boldsymbol{E}^2 \tag{10}$$

Under the two-time-scale approach, the power density in Eq. (10) was then treated as the heat source of the heat transfer phenomena to couple the electromagnetic field with the thermal field. The governing equation for heat transfer by conduction is expressed as:

$$\rho C_p \frac{\partial T}{\partial t} - \nabla \cdot \left(k \nabla T\right) = P(t) \tag{11}$$

where ρ is density, C_p is heat capacity, k is thermal conductivity, $P(t)$ is average power density, and T is temperature.

Modeling

The geometry of the RF heating system is shown in Figure 5 and 6. The electric potential of the aluminum cavity was set to 0, and a 5 kV electric potential (RMS at 27 MHz) was applied to the feeder plate. The dielectric properties of the mashed potatoes were determined from calculations in Guan *et al.* [2004], while a linear regression analysis was used to determine the relation between temperature and dielectric properties (Table 1). The electrical conductivity of circulating water were measured by a conductivity analyzer model 53 (GLI International, Milwaukee, WI, USA) at the beginning of each experiment at 23°C. In the heat transfer analysis, heat effects were only considered in the food sample domain to simplify the model. The thermal conductivity and specific heat of the mashed potatoes were measured by a KD2 Pro Thermal Properties Analyzer (Decagon Devices, Pullman, WA, USA) in triplicate at room temperature (Table 2).

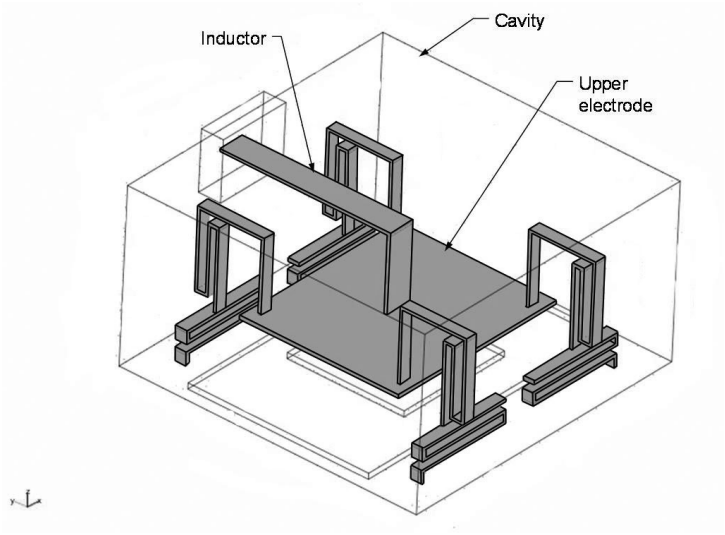

Figure 5. *Geometry model of the RF heating system.*

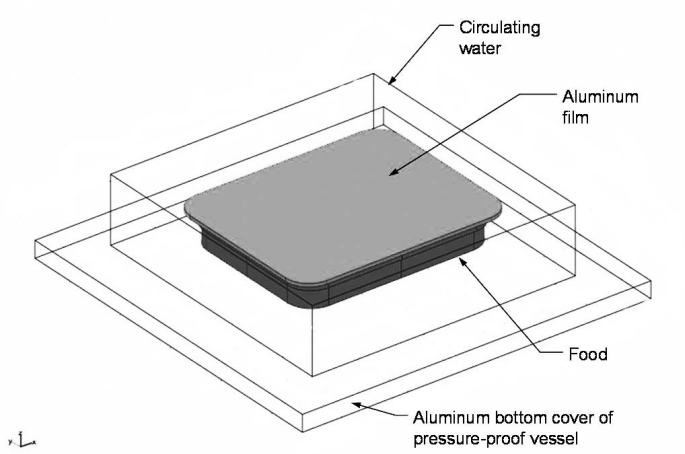

Figure 6. *Geometry model of vessel and food.*

Table 1. Summary of temperature-dielectric properties relationship of mashed potatoes samples (ε = interception + slope temperature) [Guan *et al.*, 2004].

Mashed potatoes with salt content		Interception	Slope	R^2
0.8%	ε'	84.7	0.13	0.86
	ε''	78.7	7.8	0.98
1.3%	ε'	83.3	0.14	0.85
	ε''	173.2	16.4	0.99

Table 2. Summary of mashed potatoes sample thermal properties at room temperature (mean of 3 replicates standard deviation.)

Mashed potatoes with salt content	Thermal conductivity (W/m·K)	Heat capacity (kJ/kg·K)	Approximate density (kg/m^3)
0.8%	0.545 ± 0.007	3.743 ± 0.068	1000
1.3%	0.548 ± 0.025	3.763 ± 0.112	1000

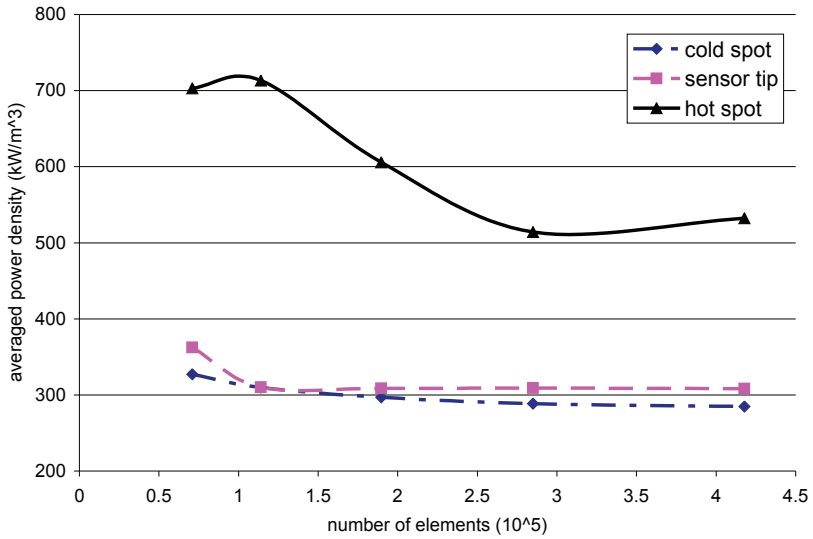

***Figure 7**. Effects of number of elements on the average power density accuracy.*

Since the flow of circulating water was ignored, no heat convection was assumed between the circulating water and sample trays. The boundary conditions for the surface of the sample trays were set to 40 °C.

Convergence study

Preliminary simulations were conducted to acquire appropriate meshing density and element numbers. The average power density at cold and hot spots and sensors were monitored to check the convergence of the simulation results. As presented in Figure 7, increasing number of elements stabilized average power density at the three locations. When the number of elements reached 417,881, there was no more than a 3.4% difference in the average power density with a 47% increase in the number of elements, indicating a stabilization of the average power density and the number of elements was reasonable to conduct further simulation.

Solution computation

The procedures for computing the solution are shown in the flow chart in Figure 8. The initial condition was assigned to the model at time zero. The FEM was then applied to obtain electric potential and electric field distributions. After the average power density was calculated based on the material properties and electric field intensity, the FEM heat transfer simulation module was used to investigate the heat generation and transfer condition. The temperature-dependant variables were modified according to the renewed temperature distribution, applied to the model, and then a renewed electric field

distribution was calculated. Iterations were continued until the final time step was reached. Variable time steps were automatic selected by simulation software to determine the optimal simulation process.

A Dell Precision 870 workstation with two Dual-Core 2.80GHz Intel® Xeon™ processors and a 12 GB memory was utilized to perform the simulation, which took about 1 h.

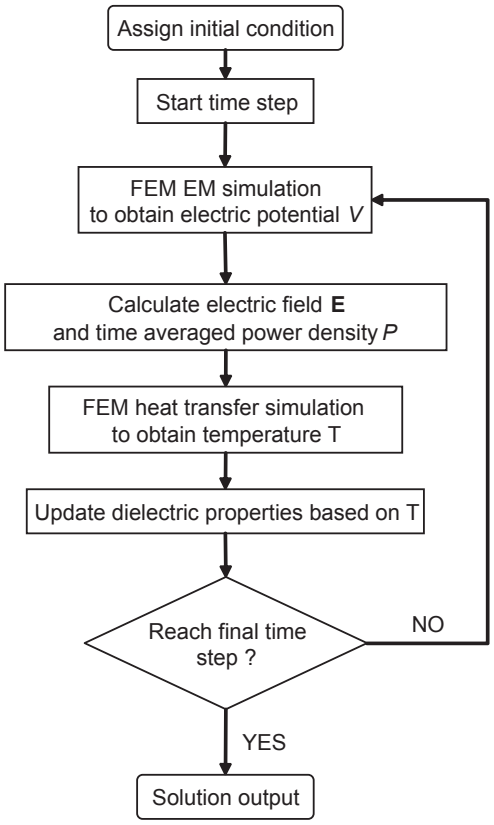

Figure 8. *Flow chart of the procedure in solution calculation.*

RESULTS

Experimental results

The heating times and final temperatures at the hot spot and cold spots and sensor tips of the mashed potato samples are summarized in Table 3. The temperature profile at the sensor tip is plotted in Figure 9, which shows that with an increase in the electrical conductivity of the circulating water, the heating rate decreased at the sensor tips. For the same temperature, the mashed potatoes with 1.3% salt content took longer to heat than those with 0.8% salt content.

Simulation results

In order to verify the simulation results, three positions in the sample were chosen to compare the numerical solutions with the experimental results. The first position was at the sensor tip, and the other two positions were at the hot and cold spots within the horizontal central layer of the sample tray, where both fiber optic sensors

Table 3. Summary of experimental heating times and final temperatures.

Mashed potatoes with salt content	Circulating water electric conductivity at 23 ºC (S/cm)	Heating time (seconds)	Temperature (ºC) at:		
			Cold spot	Hot spot	Sensor tip
0.8%	20	320	51.6	80.3	61.4
	64	390	48.6	79.5	60.3
	140	630	58.7	81.1	62.5
	220	660	55.3	79.5	58.5
1.3%	20	570	53.7	76.1	68.2
	64	660	53.0	68.1	61.2
	140	1020	54.6	70.6	60.5
	220	1200	53.2	66.8	58.4

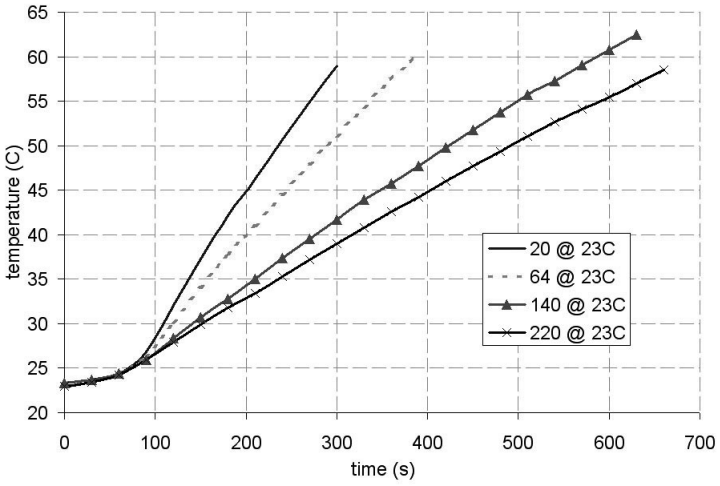

(a)

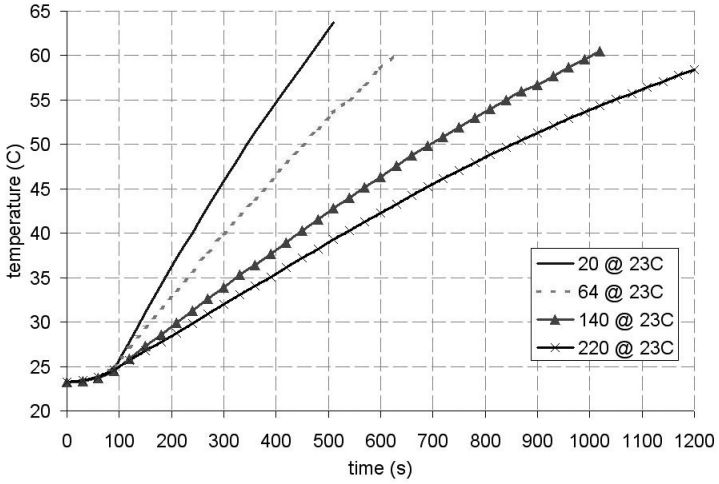

(b)

Figure 9. *Measured heating profile at the mashed potato sample sensor tips with (a) 0.8% and (b) 1.3% salt content under different circulating water (unit of water conductivity in the figure is μS/cm).*

were placed and thermal images taken to evaluate the uniformity of the heating process. Digitized by the ThermaCAM Researcher 2001, the software provided by FLIR System Inc., the thermal images provided the final heating pattern and temperatures at the hot and cold spots at the central layer of the sample tray. As shown in Figure 10, the hot spots were located at the places near the corner of the sample, and the cold spots were at the center of the sample. Temperatures at the same positions, as shown in Figure 11, were determined from the numerical solution.

Figure 12 indicates that both the increase in conductivity of the circulating water and increase in mashed potato salt content reduced the heating rates. The simulation results confirmed the temperature change trends observed in the experiments (Figure 9).

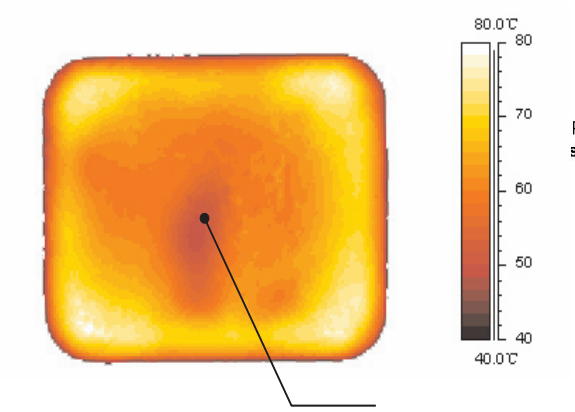

Figure 10. *Typical thermal image of the central layer of an RF-processed mashed potato sample.*

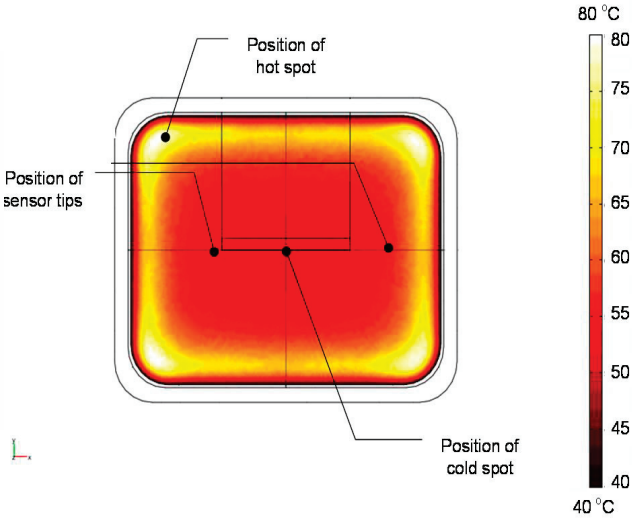

Figure 11. *Typical numerical solution of the central layer of a processed mashed potato sample*

DISCUSSION

The temperature differences, which were controlled within 11%, between the experimental and simulation results at the mashed potato cold and hot spots and sensor tips under different conditions are summarized in Table 4.

The sterilization effects of thermal treatment on food are commonly determined by sterilization value (F_0) (min) [Stumbo, 1973]:

$$F_0 = \int_0^t 10^{(T-121.1)/z}\, dt \qquad (12)$$

where T is temperature (°C), t is processing time (min), and z is 10 °C for *Clostridium botulinum* spores, which are target microorganisms in commercial thermal processes for low-acid foods (pH>4.5). Generally, a minimum safe public health sterilization value (F_0) for low-acid canned foods based on inactivation of *C. botulinum* is 3.0 min [Frazier and Westhoff, 1988]. Most food companies used a minimum process sterilization value of 5.0 min [Teixeira, 1992].

During the food sterilization process, due to the exponential nature of the sterilization calculation, a small difference at temperatures above 121 °C can introduce a large variation in sterilization value. For example, an 11% temperature difference at 121 °C represents a 13 °C temperature difference between experiment and simulation, which would cause a significant error in predicting the F_0 by simulation result. In order to guarantee the safety of commercially sterilized food, it is necessary to assure that the F_0 of the cold spot reaches the designated value. In this study, the temperature differences between the simulation and experimental at cold spots were within 5% (i.e., 6 °C at 120 °C) which limited the F_0 value error to 3 min.

Although further improvement to simulation accuracy is needed to make a completely substitution of experimentation by computer simulation possible when predicting sterilization values, simulation alone can give a reasonable indication of heating pattern and sterilization value in food packages. Computer simulation also makes it much more convenient than laboratory experimentation to adjust physical properties and equipment to improve heating uniformity during RF heating

Several reasons may account for the differences between the experimental and simulation temperature values. Measurement error is one

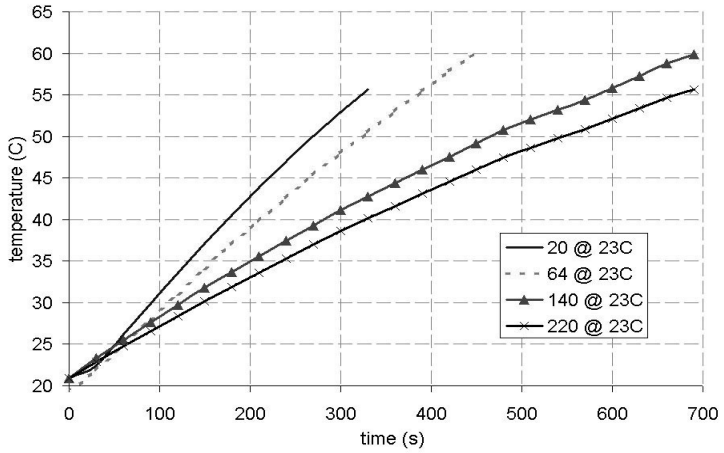

(a)

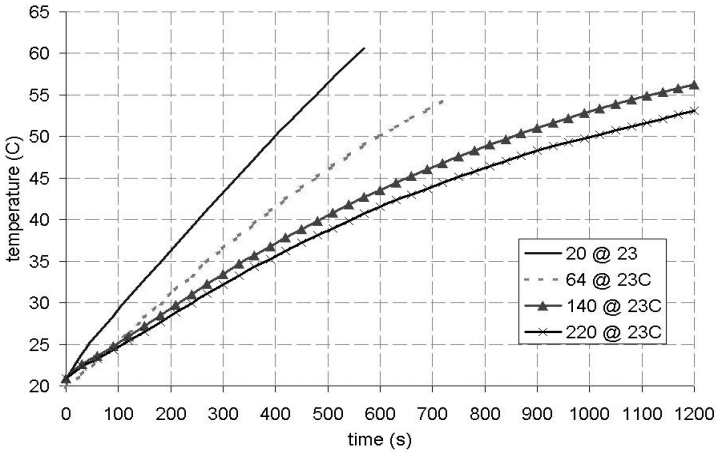

(b)

Figure 12. *Simulation results of the heating profiles at the mashed potato sample sensor tips with (a) 0.8% and (b) 1.3% salt content under different surrounding water (unit of water conductivity in the figure is μS/cm).*

Table 4. Summary of temperature differences between the experimental and simulation results.

Mashed potato salt content	Circulating water electric conductivity at 23 ºC (S/cm)	Temperature difference (ºC) at			Temperature difference (%) at:		
		Cold spot	Hot spot	Sensor tip	Cold spot	Hot spot	Sensor tip
0.8%	20	-1.4	-0.8	5.8	-2.7	-1.0	9.5
	64	-2.4	1.0	4.8	-4.9	1.3	8.0
	140	2.2	2.9	5.2	3.8	3.6	8.3
	220	-2.8	6.5	3.8	-5.1	8.2	6.4
1.3%	20	2.8	-2.9	7.6	5.2	-3.8	11.2
	64	2.5	-6.9	6.8	4.7	-10.1	11.1
	140	2.2	-2.4	7.1	4.0	-3.4	11.6
	220	0.6	-1.8	5.3	1.1	-2.7	9.1

Table 5. Simulation results of average electric field intensity and power density in water and food with different salt content.

Mashed potato salt content		0.8%	1.3%	1.8%	2.8%
Dielectric constant of mashed potato at 40 °C		90	89	79	105
Loss factor of mashed potato at 40 °C		383	817	1000	1906
Average electric field intensity in	food (kV/m)	1.1	0.5	0.5	0.2
	water (kV/m)	3.06	2.99	2.99	2.98
Average power density in	food (kW/m^3)	347	193	163	85
	water (kW/m^3)	16.4	16.1	16.1	16.1

of the distinct possibilities causing the difference, because the linear regression analysis for the temperature-dielectric properties relationship was based on mean values without considering the 10% standard deviation [Guan *et al.*, 2004]. Simplification of the model could be another reason that caused the differences. Without considering the flow of circulating water and convection between water and the sample food, the heating pattern could have been affected by the simplified heat transfer condition. Adding more details to the model would improve the precision of the simulation results, but also require much more computer memory and a faster CPU.

At RF, the loss factor of mashed potatoes increases with the rise of temperature and salt content [Guan *et al.*, 2004]. As shown in Eq. (10), the dissipated power density is proportional to the loss factor of food. Thus, if the electric field intensity, $\boldsymbol{E}$, were fixed, the increasing temperature at certain points of the food sample would lead to a rise in the local loss factor and increase heat generation at these positions, suggesting that the heating rate at positions with high temperature should be higher than those at low temperature. It is, therefore, commonly believed in the literature that a positive correlation between dielectric loss factor and temperature for foods contribute to significant runaway heating during RF heating causing overall nonuniform heating. However, both the experiments and simulations results in our studies revealed that an increase in salt content (i.e., sample loss factors) resulted in a reduced heating rate, opposite to what we originally anticipated.

In order to investigate the above stated paradox, several simulations were performed to study the electric field distributions in samples with different salt contents. During the simulation, all the physical constants (i.e., 40 °C temperature and 85.9% moisture content) of the mashed potatoes were kept the same except for the salt content, which varied from 0.8, 1.3, 1.8, to 2.8%.

According to the numerical solution summarized in Table 5, the average electric field intensity in the circulating water was relatively stable at around 3 kV/m, even though the salt content of the mashed potato changed. Since the water conductivity was fixed, the energy absorbed by the water remained steady at around 16 kW/m^3. The average electric field intensity in the sample food, on the other hand, decreased from 1.1 to 0.23 kV/m, while the loss factor increased from 383 to 1906. The sample loss factors, which are proportional to the power produced in the food, increased almost five times, but due to the dramatic decrease of electric field intensity, thermal energy conversion in the samples actually decreased. Since the average power density

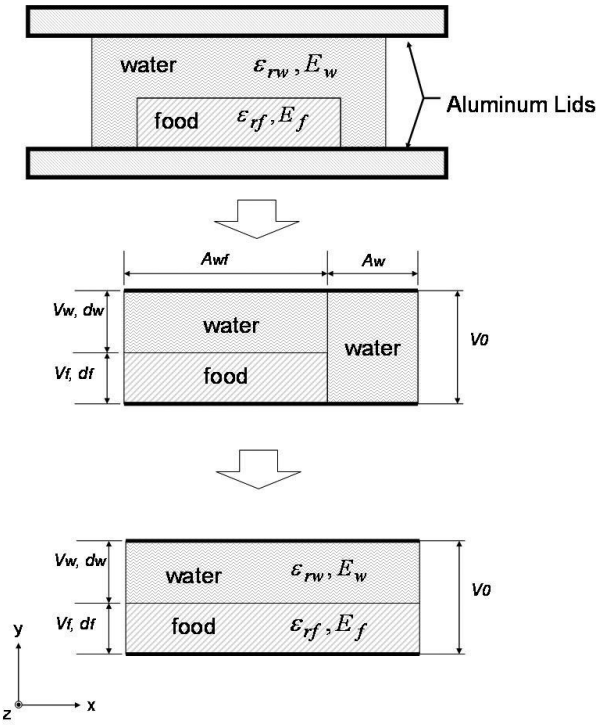

Figure 13. *Simplified diagram for calculating the electric field distribution inside the RF heating system.*

dropped from 347 to 85 kW/m^3, the heating rate declined with the rise in salt content of the mashed potatoes.

To better understand these phenomena, a simplified analytical calculation was conducted using an RF heating system with only a pressure-proof vessel, circulating water, and food (Figure 13).

The electric potential between the two metal plates can be calculated from:

$$V_0 = d_w E_w + d_f E_f \tag{13}$$

where E_w is the electric field intensity in circulating water, E_f is the electric field intensity in food, d_w is the thickness of water, and d_f is the thickness of food.

Assuming the electrostatic field, the electric field is uniform in the material and with only considering the electric field in y-direction (as shown in Figure 13), the boundary condition at interface between water and food is:

$$\varepsilon_w E_w = \varepsilon_f E_f \tag{14}$$

where ε_w is the is the permittivity of circulating water, and ε_f is the is the permittivity of food. According Eq. (8), (9), and (14) can be rewritten as:

$$\varepsilon'_{rw} E_w = \varepsilon'_{rf} E_f \tag{15}$$

where ε'_{rw} is the dielectric constant of circulating water, and ε'_{rf} is the dielectric constant of food.

Combining Eqs. (13) and (15),

$$E_f = \frac{V_0 \varepsilon'_{rw}}{\varepsilon'_{rw} d_f + \varepsilon'_{rf} d_w} \tag{16}$$

Finally with considering about Eq. (10), the power density inside the food can be approximated to

$$P_f \approx \omega \varepsilon_0 \varepsilon''_{rf} V_0^2 \left[\frac{\varepsilon'_{rw}}{\varepsilon'_{rw} d_f + \varepsilon'_{rf} d_w} \right]^2 \tag{17}$$

Table 6. Comparison between simulation and analytical results of average power density in food with different salt content.

Mashed potato salt content		0.8%	1.3%	1.8%	2.8%
Dielectric constant of mashed potato at 40 °C		90	89	79	105
Loss factor of mashed potato at 40 °C		383	817	1000	1906
Average power density in food (kW/m^3)	Simulation	347	192.5	162.5	85
	Analytical	366	179	148	79

The analytical calculations based on Eq. (17), as shown in Table 6, present a clear similarity to the simulation results of the average electric field intensity and power density in water and mashed potato with different salt contents. According to Eq. (17), the power density inside the food is not only proportional to its loss factor, but also influenced by the food thickness, circulating water, and dielectric properties.

CONCLUSIONS

Both experimental and simulation results indicated that with an increase of water electric conductivity or salt content (loss factor) in mashed potato samples, their heating rate decreased. The simulation results further demonstrated that although the dissipated power in the mashed potatoes was proportional to their loss factor, the decreased electric field intensity caused by the increased loss factor not only compensated for the influences brought by the increase in loss factor, but actually reduced the dissipated power. According to our analytical calculations, the power density inside mashed potatoes is not simply proportional to their dielectric loss factor, but influenced by the thickness of mashed potato and circulating water and their dielectric properties and electric conductivity, respectively. Although several assumptions affected the simulation accuracy, a reasonable indication of mashed potato heating pattern and heating rate was obtained. Computer simulation has the potential to further improve similar simulations and aid the construction and modification of RF heating systems.

ACKNOWLEDGMENT

The authors appreciate financial support from the US Army Natick Soldier Center and WSU Agricultural Research Center. We also thank Strayfield Ltd., UK, for free leasing of a RF system, and Rexam Containers, Union, MO, USA, for the donation of polymeric trays.

REFERENCES

Baginski, M., Broughton, R., Hall, D., and Christman, L. (1990). "Experimental and Numerical Characterization of the Radio-Frequency Drying of Textile Materials (II)." *Journal of Microwave Power and Electromagnetic Energy*, 25(2), pp.104-113.

Balanis, C.A. (1989). Advanced Engineering Electromagnetics, John Wiley & Sons, New York, NY, USA.

Banwart, G.J. (1989). Basic Food Microbiology, Van Nostrand Reinhold, New York, NY USA.

Barber, H. (1983). Electroheat, Sheridan House, Inc., Dobbs Ferry, New York, NY, USA.

COMSOL (2005). Electromagnetics Module User's Guide, COMSOL Multiphysics, Burlington, MA, USA.

Chan, T.V.C.T., Tang, J.M., and Younce, F. (2004). "Three-Dimensional Numerical Modeling of an Industrial Radio Frequency Heating System using Finite Elements." *The Journal of Microwave Power and Electromagnetic Energy*, 39(2), pp.87-105.

Frazier, W.C. and Westhoff, D.C. (1988). Food Microbiology. 4th ed. McGraw-Hill, New York, NY, USA.

Guan, D., Cheng, M., Wang, Y., and Tang, J. (2004). "Dielectric Properties of Mashed Potatoes Relevant to Microwave and Radio-Frequency Pasteurization and Sterilization Processes." *Journal of Food Science*, 69(1), pp.E30-E37.

Haus, H. A. and Melcher, J. R. (1989). Electromagnetic Fields and Energy, Prentice Hall, Englewood Cliffs,

NJ, USA

Luechapattanaporn, K., Wang, Y., Wang, J., Al-Holy, M., Kang, D.H., Tang, J., and Hallberg, L.M. (2004). "Microbial Safety in Radio Frequency Processing of Packaged Foods." *Journal of Food Science*, 69(7), pp.M201-M206.

Luechapattanaporn, K., Wang, Y.F., Wang, J., Tang J.M., Hallberg, L.M., and Dunne, C.P. (2005). "Sterilization of Scrambled Eggs in Military Polymeric Trays by Radio Frequency Energy." *Journal of Food Science*, 70(4), pp.E288-E294.

Marshall, M.G. and Metaxas, A.C. (1998). "Modeling of the Radio Frequency Electric Field Strength Developed during the RF Assisted Heat Pump Drying of Particulates." *Journal of Microwave Power and Electromagnetic Energy*, 33(3), pp.167-177.

Meredith, R., ed. (1998). Engineers Handbook of Industrial Microwave Heating, The Institution of Electrical Engineers, London, UK.

Neophytou, R.I. and Metaxas, A.C. (1998). "Combined 3D FE and Circuit Modeling of Radio Frequency Heating Systems." *Journal of Microwave Power and Electromagnetic Energy*, 33(4), pp.243-262.

Neophytou, R.I. and Metaxas, A.C. (1999). "Combined Tank and Applicator Design of Radio Frequency Heating Systems." *IEE Proceedings Microwaves, Antennas, and Propagation*, 146(5), pp.311-318.

Priestley, R.J. (1979). Vitamins. In: Priestley, R.J., ed. Effects of Heating on Foodstuffs, pp.121-156. Applied Science Publishers, Essex, UK.

Sadiku, M.N.O. (2001). Elements of Electromagnetic, 3rd edition, Oxford University Press Inc., New York.

Stumbo, C.R. (1973). Thermobacteriology in food processing, 2nd edition, Academic Press, London.

Teixeira, A. (1992). Thermal Process Calculation. In: Heldman D.R. and Lund, D.B., eds. Handbook of Food Engineering, Marcel Dekker, New York, NY, USA.

Wang, Y., Wig, T.D., Tang, J., and Hallberg, L.M. (2003a). "Sterilization of Foodstuffs Using Radio Frequency Heating." *Journal of Food Science*, 68(2), pp.539-544.

Wang, Y.F., Wig, T.D., Tang, J.M., and Hallberg, L.M. (2003b). "Dielectric Properties of Foods Relevant to RF and Microwave Pasteurization and Sterilization." *Journal of Food Engineering*, 57(3), pp.257-268.